PROCEEDINGS B

rspb.royalsocietypublishing.org

Research

Cite this article: Blanke A, Watson PJ, Holbrey R, Fagan MJ. 2017 Computational biomechanics changes our view on insect head evolution. *Proc. R. Soc. B* 20162412. http://dx.doi.org/10.1098/rspb.2016.2412

Received: 3 November 2016
Accepted: 9 January 2017

Subject Category:
Evolution

Subject Areas:
evolution, biomechanics

Keywords:
mouthpart, muscle, finite-element analysis, multibody dynamics, Palaeoptera problem

Author for correspondence:
Alexander Blanke
e-mail: a.blanke@hull.ac.uk

Electronic supplementary material is available online at rs.figshare.com.

THE ROYAL SOCIETY PUBLISHING

Computational biomechanics changes our view on insect head evolution

Alexander Blanke, Peter J. Watson, Richard Holbrey and Michael J. Fagan

Medical and Biological Engineering Research Group, School of Engineering, University of Hull, Hull HU6 7RX, UK

AB, 0000-0003-4385-6039

Despite large-scale molecular attempts, the relationships of the basal winged insect lineages dragonflies, mayflies and neopterans, are still unresolved. Other data sources, such as morphology, suffer from unclear functional dependencies of the structures considered, which might mislead phylogenetic inference. Here, we assess this problem by combining for the first time biomechanics with phylogenetics using two advanced engineering techniques, multibody dynamics analysis and finite-element analysis, to *objectively* identify functional linkages in insect head structures which have been used traditionally to argue basal winged insect relationships. With a biomechanical model of unprecedented detail, we are able to investigate the mechanics of morphological characters under biologically realistic load, i.e. biting. We show that a range of head characters, mainly ridges, endoskeletal elements and joints, are indeed mechanically linked to each other. An analysis of character state correlation in a morphological data matrix focused on head characters shows a highly significant correlation of these mechanically linked structures. Phylogenetic tree reconstruction under different data exclusion schemes based on the correlation analysis unambiguously supports a sistergroup relationship of dragonflies and mayflies. The combination of biomechanics and phylogenetics as it is proposed here could be a promising approach to assess functional dependencies in many organisms to increase our understanding of phenotypic evolution.

1. Introduction

The so-called 'Palaeoptera problem'—the unclear relationships of dragonflies (Odonata), mayflies (Ephemeroptera) and all other winged insects (Neoptera)—was identified as one of the few remaining challenges in deep-level insect systematics [1]. The Palaeoptera problem is of special interest, because it also relates to the evolution of insect flight which evolved approximately 400 Ma [2,3]. Owing to the wingless outgroup silverfish, it is unclear how the insect flight mechanism evolved, therefore, resolving early winged insect relationships would help to further our understanding of the evolution of insect flight [4].

Previous attempts [5–8], and more recently even large and sophisticated transcriptomic studies [3] have failed to resolve the Palaeoptera problem unambiguously. Other approaches focusing on an increase in the signal-to-noise ratio within diverse molecular datasets have also produced inconclusive results [9].

One possible solution to assess the Palaeoptera problem is to increase our understanding of the functional relationships of characters used in phylogenetics in an *objective* way, for example, through biomechanical testing. Revealing such functional character linkages with regards to phylogeny can point towards problems with the way morphologies are coded in datasets, in addition to increasing our general understanding of shape evolution under mechanical constraints or triggers. In the context of the Palaeoptera problem, disagreement for the most frequently favoured hypotheses Metapterygota (Odonata + Neoptera), and Palaeoptera (Odonata + Ephemeroptera) is derived partly from head morphology. Metapterygota are supported by the similar anterior mandibular ball-and-socket articulation and the loss of mandibular

muscles [10,11], while Palaeoptera are supported by the similar structure of the maxillary lacinia, characters related to the antennae, and the loss of a labial muscle [12].

Until recently, however, testing objectively for character linkage in insect head structures was impossible due to a lack of sufficiently detailed biomechanical models. We have developed a biomechanical workflow able to handle the large three-dimensional models needed for analysis [13–15] and with the advent of synchrotron radiation micro-computed tomography (SR-μCT, [16,17]) it is now possible to generate extremely detailed three-dimensional models of insects [12,18,19] which can be imported into mechanical simulation software to study the mechanical loading and strains occurring in insect heads. These strain patterns then allow an assessment of the degree of mechanical interdependency within the insect head and thus can serve as an objective measure of character linkage. Testing these linked characters for pairwise correlation based on the mechanical data could reveal the influence of function on phylogeny.

2. Experimental procedures

(a) Synchrotron radiation micro-computed tomography and segmentation

We built a three-dimensional model of the damselfly *Lestes virens* (electronic supplementary material, figure S1) derived from high-resolution SR-μCT performed at the Deutsches Elektronen Synchrotron (DESY, Hamburg, Germany). After fixation in Bouin solution [20] which usually leads to a shrinkage of soft tissue of approximately 5% [20], the sample was washed in 70% EthOH, critical point dried (Model E4850, BioRad), and mounted on beamline-specific specimen holders. SR-μCT was performed at beamline DORIS III/BW2 with a monochromatic X-ray beam at 8 keV photon energy, 3.4× magnification and an isotropic voxel size of 4.7 μm. We designated the voxels (segmentation) of the reconstructed image stacks to the head capsule, mandibles and mandibular muscles using the open-source segmentation software ITK-SNAP [21]. The segmentation was done using a combination of semi-automatic active contour segmentation and manual correction of the semi-automatic segmentation in three orthogonal planes. Owing to the superior quality of the image stacks, manual correction of the automatic segmentation was only necessary at the transitions from head capsule to other chitinous parts such as antennae.

(b) Multibody dynamics modelling

Apart from a detailed three-dimensional geometric model of head, mandibles and muscles, precise information on muscle and joint forces is needed to perform a biologically realistic mechanical analysis (electronic supplementary material, figures S1 and S2). As it is currently impossible to measure the joint reaction forces at the mandibles of insects, we used multibody dynamics analysis (MDA; electronic supplementary material, figure S5), an engineering tool which is becoming increasingly popular for the analysis of skull biomechanics in vertebrates [22–25]. MDA outputs joint reaction and muscle forces which can subsequently be used as the input for finite-element analysis (FEA; see below).

An MDA model was created by importing volumetric models of the head capsule and mandibles into ADAMS 2013 (MSC Software Corp. USA). The cranium was constrained in all degrees of freedom, and spherical anterior and posterior joints defined between the cranium and the mandibles so that the mandibles were modelled as movable parts relative to the cranium. Each muscle was modelled through a series of strands in order to replicate the pennation observed in the microCT data. It has been shown that the potential groundplan mandible muscle equipment of dragonflies is composed of seven muscles [12,26], and the chosen damselfly *Lestes virens* shows this muscle pattern. The M. hypopharyngomandibularis was not considered in this model since it is a small muscle connecting two movable parts (mandible and a hypopharyngeal sclerite). Therefore, the influence of this muscle cannot be modelled with certainty. Consequently, the MDA model contained six muscles which were represented through a total of 30 strands on each side of the head (electronic supplementary material, figure S2).

The maximum intrinsic force of each muscle was estimated as: maximum cross-sectional area times muscle stress. Each muscle cross-sectional area was determined from the microCT data by measuring the attachment area at the head exoskeleton. As most mandibular muscles, and in particular the main adductor muscle, have a fan-like geometry, measurement at the attachment site represents the most accurate and repeatable approach to ensure an orientation of the plane of measurement perpendicular to each region of the respective muscle, to capture the widest cross-sectional area and to avoid measurement errors due to potential shrinkage. Reported insect muscle stress values vary widely, ranging from 13.7 to 49 N cm^{-2} measured for single myofibrils [27–29]. Because specific data for this particular insect is not available, a standard value of 25 N cm^{-2} was used for the intrinsic muscle stress in this simulation [30,31]. Results from the simulation of muscle forces are accordingly as shown in the electronic supplementary material, figure S5.

Each muscle strand was activated using a dynamic geometric optimization (DGO) method, which calculates the force within a strand based upon its orientation, in order to cause the mandible to follow a specific motion (for a detailed description of the DGO method, see [32]). The DGO was employed to initially simulate jaw opening to a gap that was sufficient to enable a food particle to be placed at the mid-point between the mandibles (electronic supplementary material, figure S2). During the subsequent closing phase, the mandibles contacted the food particle and generated a bite force. The predicted maximum bite force of 0.39 N was 0.08 N higher than the maximum measured bite force (0.31 N) in a similarly sized different dragonfly species [33], thus it can be assumed that the MDA model was predicting physiologically reasonable joint reaction and muscle forces as was also shown in former sensitivity studies [34,35]. The MDA model is deposited under Dryad accession number DIO XXXXX. Q1

(c) Finite element analysis (FEA)

We used the open-source finite-element solver VOX-FE2 [13] for the analysis of stress and strains in the head. A graphical user interface developed as a plugin for

PARAVIEW (v. 4.1.0, www.paraview.org; plugin available from http://sourceforge.net/projects/vox-fe) was used to generate the FE mesh and define the muscle forces and model constraints. The segmented head geometries were exported from ITK-SNAP and converted in PARAVIEW into an FE mesh of 9.7 million hexahedral elements by direct voxel conversion. Joint reaction forces at the anterior and posterior joints were obtained from the MDA model simulation. Muscle loads were applied as distributed forces in the model to reflect their wide attachment sites *in vivo* ('Load case A'; electronic supplementary material, figure S3*b*). Reaction forces at the mandible joints, bite force and muscle forces were applied according to the MDA calculations. While these forces are exactly those required to place the head in static equilibrium, rounding errors in the solution phase means that additional constraints must be defined on the FE model to prevent any rigid body motion. Three points were chosen at the edges of occipital foramen (the opening of the head to the thorax), two at the lateral sides and one at the dorsal side. All three nodes were constrained in all directions.

Young's modulus (E) and Poisson's ratio (ν) of cuticle where taken from own measurements reported in other studies [36] and are in agreement with the literature data (here: $E = 7.3$ GPa, $\nu = 0.3$ [37,38]).

To determine whether strains in particular parts of the head structure during biting are generated predominantly by the joint reaction forces or by the muscle forces, separate analyses were run either with the main mandibular adductor muscle modelled as a 12 stranded muscle rather than a distributed force ('Load case B'; electronic supplementary material, figure S3*c*), or without the forces of this muscle ('Load case C'; electronic supplementary material, figure S3*d*). Note that load case C is a non-physiological loading scenario and used solely to investigate the relative importance of each applied load. The FEA model is deposited under Dryad accession number DIO XXXXX.

(d) Further analysis of the mechanically linked characters

To explore the influence of the mechanically linked morphological characters on current phylogenetic estimates, we tested them for pairwise character correlations using the 'fitPagel' test within the 'phytools' package in R [39] which depends on R packages 'ape' [40,41] and 'geiger' [42]. The test is based on the correlation test for discrete data proposed by Pagel [43] taking into account branch lengths and phylogeny of an independent tree inference. To carry out this test, we considered a morphological data matrix (electronic supplementary material, table S1) obtained from the literature which is focused on the analysis of deep-level insect relationships using head structures [12,44]. For testing against a phylogeny, we considered the large-scale transcriptomic analysis carried out by Misof *et al*. [3] as this constitutes the most up-to-date and rigorous estimate of diversification times in insects (and therefore of branch lengths which are required for the Pagel test). The original phylogeny [3] was pruned in R to reduce it to the same number of taxa like in the morphological matrix. Since the Palaeoptera problem received no support in the Misof *et al*. [3] study, we also tested the morphological characters against the major published alternative hypotheses Metapterygota and Chiastomyaria by realigning the Misof *et al*.[3] phylogeny accordingly, keeping the branch lengths and the rest of the topology identical. Pagel's correlation method only works on binary data [43]. Therefore, we recoded several characters within the original character matrix to fit this prerequisite. These are the following characters for our subsample: orientation of head (character 1), areas of origin of antennal muscles (35) and anterior mandibular joint (70). Refer to the electronic supplementary material, tables S1 and S2 for a full overview on the original and the recoded subset matrix.

We subsequently tested those characters which code for head capsule and mandible structures in the widest sense (e.g. including also all mandibular and tentorial muscles; electronic supplementary material, table S2). Owing to this, the final Pagel test 'all-versus-all' resulted in 462 pairwise tests of 31 head and mandible characters for each hypothesis (Palaeoptera, Metapterygota and Chiastomyaria). For the final matrix reduction, we only considered those characters which showed a highly significant correlation ($p < 0.0005$) in each pairwise test for *all* three hypotheses (electronic supplementary material, table S3). The results were visualized using the 'chordDiagramFromDataFrame' function in the 'circlize' package of the R software environment [45]. To prevent an artificial downweighting of character complexes, we only excluded one character of each correlated character pair for the subsequent tree reconstructions. To test the effect of excluding different parts of character pairs found in the correlation analysis, we generated four reduced character matrices based on the correlative data, one basically excluding the joint characters and keeping the mandible muscle characters (which were retrieved as highly interconnected; Matrix 1; electronic supplementary material, dataset S1). In the second matrix, we excluded the joint characters and kept the characters related to the tentorium (Matrix 2; electronic supplementary material, dataset S2), the third matrix was reduced by the mandible muscle characters while we kept the joint characters (Matrix 3; electronic supplementary material, dataset S3), while the fourth matrix was reduced vice versa to the second matrix (Matrix 4; electronic supplementary material, dataset S4). Finally, the fifth matrix was reduced by all characters retrieved as highly significant (electronic supplementary material, dataset S5). These five morphological data matrices were used for phylogenetic analysis using maximum parsimony in TNT [46] and Bayesian inference implemented in MR BAYES 3.2.2. [47] using established procedures [48,49].

3. Results

The performance of the FEA head models were examined by considering the first and third principal strain distributions (ε1 and ε3, respectively), which correspond to the most tensile and most compressive strains at each point of the model. ε1 and ε3 distributions show areas of highest strain at the mandible joints, which are each composed of an anterior and posterior ball-and-socket joint in Odonata and Neoptera (figure 1*a*,*b*; electronic supplementary material, movie S1), and along certain ridges, which are regions of thickened cuticle (figure 1*c*–*e*; electronic supplementary material, figure S4 and movie S1). In particular, strain (ε1 + ε3) near the anterior mandibular joints is distributed along the invagination of the anterior tentorial pits (externally visible invagination areas of the endoskeleton), the subgenae

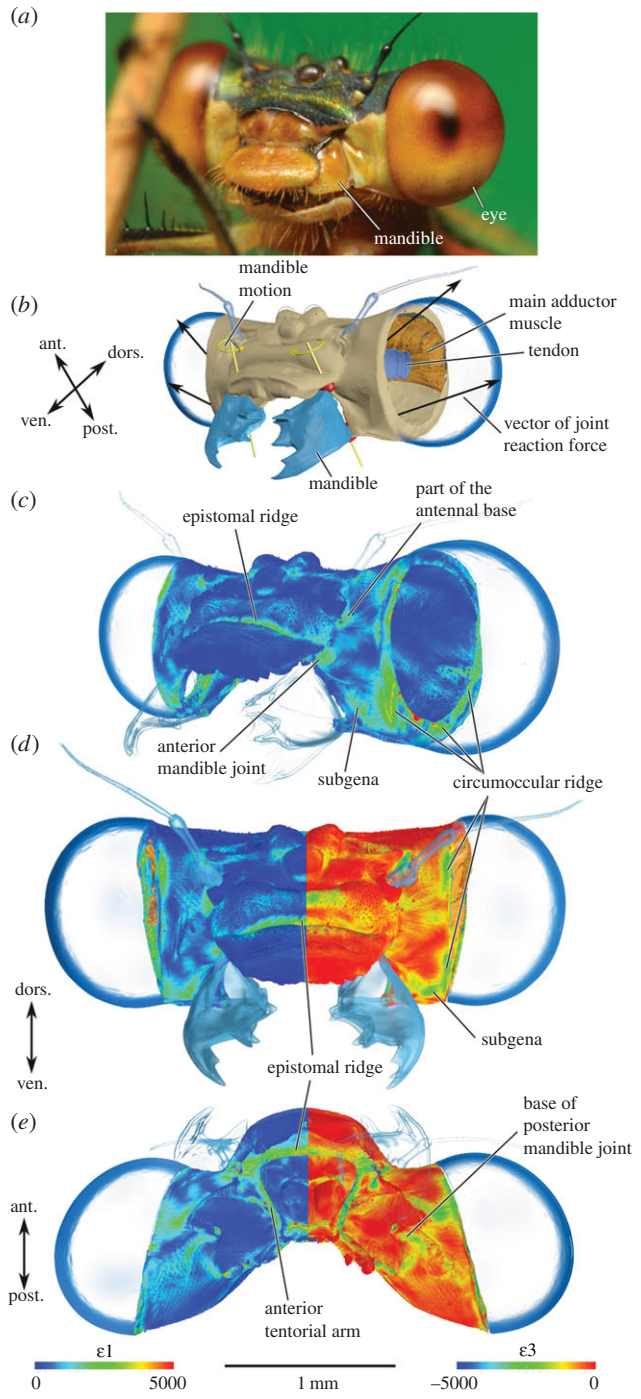

Figure 1. FEA of the head capsule of *Lestes virens* for a typical load case during biting. (*a*) Overview of the outer morphology of an exemplary damselfly head (*Lestes sponsa*, Zygoptera, Odonata) to facilitate orientation. (*b*) Three-dimensional reconstruction showing mandible joint points (red), principal mandible motion (yellow) and a part of the main adductor muscle (orange). Note the mandible motion around a fixed axis of rotation. Black arrows are the joint reaction force vectors derived from the MDA, frontolateral view. (*c*) First principal strain (ε1) during a typical load case in frontolateral view, phylogenetically relevant structures are indicated. (*d*) First (ε1, left) and third principal strain (ε3, right) in frontal view. (*e*) First (ε1, left) and third principal strain (ε3, right) in ventral view. Values are in microstrain (μS), eye and mandibles are shown to facilitate orientation. Scale bar only valid for (*d* + *e*).

(a lateral region of the head capsule above the mandibles), dorsally towards the circumantennal ridge and along the epistomal ridge, a ridge spanning anteriorly over the head from one anterior tentorial pit to the other (figure 1*c*,*d*). Parts of the cephalic endoskeleton, basically a hard, X-shaped structure connected to the inside of the head which is called tentorium in insects, equally show high strain values mainly towards the anterior mandibular joints and towards the central part of the tentorium (called the corpotentorium; figure 1*e*). Specifically, the anterior tentorial arms, which are two arms of the 'X' connected to head, and the dorsal tentorial arms (connected to the upper parts of the head) show high strain under biting load.

ε1 and ε3 at the posterior mandibular ball-and-socket joints are distributed mainly over the subgenal ridge (the ridge separating the subgena from the rest of the head) and a ridge originating at the posterior joint running in posterior direction towards the circumocular ridge (which is an internal ridge enclosing the eye; figure 1*e*; electronic supplementary material, movie S1). Strain levels at the circumocular ridge are also high despite these structures being located comparably far away from the mandibular joints (figure 1*c*,*d*; electronic supplementary material, figure S4).

To detect whether the observed strain patterns are really connected to the biting action of the mandibles, we additionally ran artificial loading scenarios by modifying (Load case 'B') or excluding (Load case 'C') the forces of the mandibular muscles, which are mainly attached to the backside of the head and the tentorium, from the simulation.

When the main mandibular adductor was modelled as a simple 12 stranded muscle (Load case 'B') rather than being distributed over the actual muscle attachment area (Load case 'A') the FEA predicted the same strain at the constraint points (electronic supplementary material, figure S2), which is a good indicator that the applied loading is still close to equilibrium. However, upon closer inspection of the muscle attachment areas at the back of the head, the strain patterns are clearly unrealistic, since the strain is highly localized to the muscle attachment points (electronic supplementary material, figure S5).

In load case 'C', mandibular muscles were excluded from the analysis so that only the joint reaction loading forces were applied to the model. Again this resulted in similar overall strain patterns for the structures investigated in our study, i.e. those used as morphological characters. But, as expected, notable differences were observed in the strain distribution at the back of the head near the occipital foramen where the constraints were applied in order to prevent free body movement (electronic supplementary material, figure S5). It is important to stress the fact that both load cases (B + C), but especially case 'C' without muscle forces, constitute biologically unrealistic boundary conditions for the FE analyses. A number of studies showed that unrealistic force simulation can even lead to different strain patterns thus affecting the conclusions drawn [34,35,50,51]. Based on these results, we conclude that the conspicuous strain pattern seen in load case A is generated primarily by the forces acting at the mandible joints, i.e. the biting motion of the mandibles.

To explore whether the mechanical linkage (expressed as strain patterns) between the mentioned head capsule structures is detectable within data used for phylogenetic reconstruction, we investigated a character matrix focused on head characters for character correlation based on our mechanical results (see Experimental procedures). In total, 272 (19.6%) of the 1386 tested head character pair combinations show a highly significant correlation to each other (figure 2). Among these combinations, head ridges,

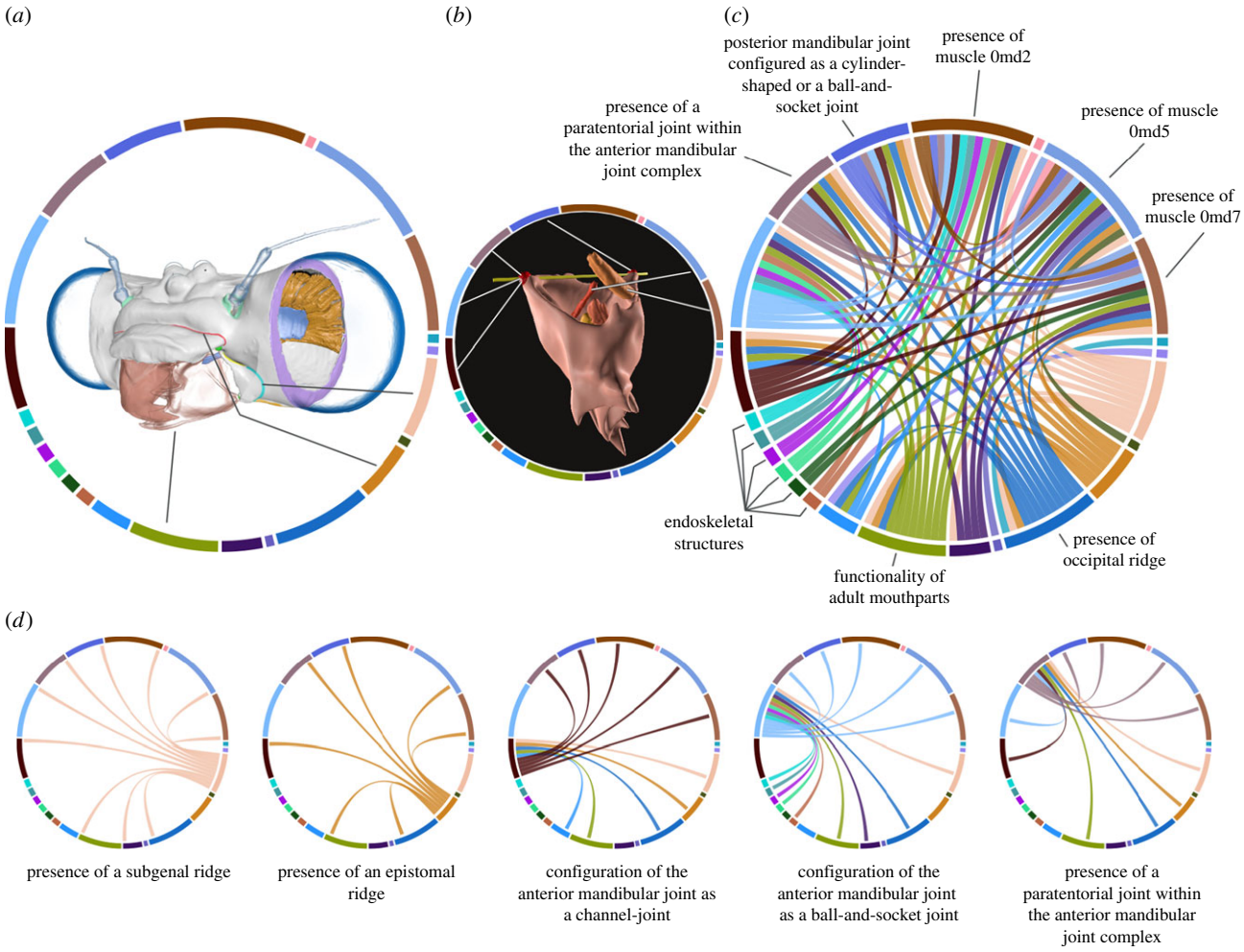

Figure 2. Results of the pairwise correlation test of the character matrix subset focused on head and mandible structures. (*a*) Location of the characters on a three-dimensional model of the head of *Lestes virens*. (*b*) Detail of (*a*) showing the location of some of the mandibular characters. (*c*) Character interdependencies. Note that only highly significant ($p < 0.0005$) correlations are shown, the tested submatrix consisted of a total of 31 characters. For a full overview including non-significant correlations, see the electronic supplementary material, figure S3 and tables S1–S3. (*d*) Exemplary circular plots extracted from (*c*) showing the interdependencies of a subset of characters. For a full overview of all single circular plots, see the electronic supplementary material, figure S3.

in particular the subgenal, the occipital and the epistomal ridge, the endoskeleton, both mandibular joints and a number of mandibular muscles (figure 2*c*) show a high degree of correlation with other head characters or to each other. Closer examination of the detailed dependencies (figure 2*d*; electronic supplementary material, figure S6) reveals that the presence of a subgenal and an epistomal ridge each is correlated with the presence of an anterior joint. In turn, the anterior mandibular joint shows correlations with the configuration of a number of endoskeletal characters and the presence of several intramandibular muscles. These muscles are in turn correlated to each other.

We used the results from this correlation test of 'all-versus-all' characters for a reduction of the largest published character matrix for insect heads [12,44]. In each of the resulting four scenarios of character exclusion, we account for different mechanically linked character complexes under the premise to prevent double-downweighting due to exclusion of character pairs. Refer to the material and methods section and electronic supplementary material, appendix SI electronic supplementary material, table S1–S3 and dataset S1–S5 for further details on character exclusion. All trees based on the different reduced datasets unambiguously support the Palaeoptera hypothesis, a sistergroup relationship of dragonflies and mayflies (figure 3).

4. Discussion

Using a highly detailed (approx. 10 M elements) finite-element model of an approximately 3 mm wide insect head allowed the visualization of the mechanical relationship of certain head structures under load for the first time. The analysis shows that the strain arising in the head from biting is supported by the subgenal, epistomal, circumoccular and occipital ridges and the anterior and dorsal tentorial arms in the anterior part of the endoskeleton (figure 1). Closer inspection furthermore reveals that the proximity of the subgenal ridge with the circumoccular ridge supports the strain generated by the two ball-and-socket mandibular joints (figure 1). Combinations of these morphological structures have been used previously to infer the relationships of basal winged insects [10–12,44], but this analysis now clearly establishes that they are in fact mechanically connected to each other. It appears that the evolution of a fixed axis of rotation of the mandible, as it is present in basal winged insects except mayflies, also selected for a strong subgenal and epistomal ridge and stronger endoskeletal arms, and coincided with the trend of a loss or reduction of the small tentoriomandibular muscles in winged insects [52]. Evidence from the present (table in electronic supplementary material, figure S2) and other studies [33,53] indicates that the small

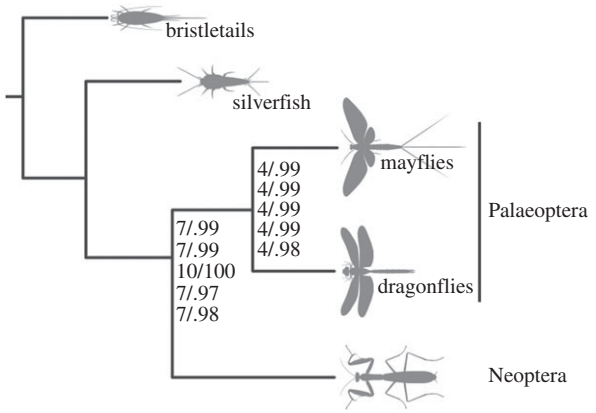

Figure 3. Phylogenetic reconstruction using different exclusion scenarios of mechanically correlated characters. Support values are indicated at the nodes. First node value: Bremer support; second node value: posterior probabilities.

tentoriomandibular muscles contribute less than 3–6% of the force of the main adductor muscle (additionally with a sub-optimal attachment geometry) in dragonflies and this is probably also the case for other winged insects where lineage-dependent (electronic supplementary material, table S1) remnants of these muscles exist with a similar geometrical configuration as in dragonflies [52]. Apparently, the large mandibular adductor muscle M. craniomanibularis internus provides the main force proportion which is in agreement with the large head volume this muscle occupies in those insects which use their mandibles for feeding [54,55], securing mating rights [56,57] or other functions where high or quickly released bite forces are advantageous. In primary wingless insects such as silverfish and bristletails, the tentoriomandibular muscles are well developed which is probably correlated with the different configuration of the mandible joints and more degrees of freedom of the mandibular movement in these lineages.

The structural changes in ridge and joint configuration are believed to result in stronger biting capabilities in Odonata and Neoptera, and were formerly used as a strong argument in favour of the Metapterygota (Odonata + Neoptera) hypothesis [10,11,58]. These statements have thus far not been investigated with an objective testing scheme focused on the mechanical linkage of morphological characters, since it proved to be extremely difficult to experimentally investigate the mechanics of insect heads under load due to their small size. MicroCT datasets combined with the methodological approach presented here, clearly show functional linkage in joint and ridge structures in these winged insects. Indeed, the uniformity of structures associated with the mandibular joint, the main mandibular muscles and certain ridges, such as the subgenal ridge, across the winged insects considered here is striking and the correlation analysis of the available morphological data matrix supports that this uniformity of character states generates biasing phylogenetic signal (figure 2). Other recent datasets additionally indicate that traditional mandibular performance measures, such as the mechanical advantage [59–61], are similar across distantly related lineages such as dragonflies [36] and cockroaches [62] despite their varying food preferences. However, many more species from different lineages need to be studied to corroborate this idea of similar mechanical performance despite varying food preferences.

Excluding subsets of the above-mentioned problematic characters according to the found character correlations supports the Palaeoptera hypothesis (figure 3). The ancestral mode of insect flight thus most probably was an indirect system with the flight muscles attached to the thorax as shown by mayflies and all other winged insects except dragonflies. The direct flight mechanism accordingly is likely a derived condition which most probably evolved only once in the common ancestor of dragonflies. Supporting characters (i.e. synapomorphies) for the Palaeoptera clade are the length ratios of the antennal segments, the absence of antennal circulatory organs, the presence of dentisetae at the maxillae and the absence of a muscle in the labium. Other studies focused on a mathematical detection of convergence equally support these characters as synapomorphies [63].

(a) Biomechanics allows for the objective study of character linkage in insects

Apart from insect heads, character linkage has also been assessed in a range of plant [64–66] and bird character complexes [67,68]. While the three earlier studies used 'classical' character mapping on a molecular phylogeny, the other two formally assessed potential confounding signals within the character state distribution, an approach also used for insect heads [63]. The problematic issue mentioned in all of these studies is the uncertain functional relationship between characters since the methods used only test for compositional bias within a character state distribution [67] and not directly for functional interdependencies.

Another potential drawback of mathematical concerted convergence testing is that it is not possible to reveal the influence of retained (plesiomorphic) character states that do not undergo adaptive character state changes [69–71]. Mathematical concerted convergence analysis only tests for conspicuous patterns of character state *changes*. However, plesiomorphic characters might also influence state changes in other characters [72,73]. In this context, biomechanical testing of character interdependency is an approach to better understand both directional (resulting in autapomorphies) and stabilizing (resulting in maintained plesiomorphies) elements of selection pressures acting on the mechanical evolution of structures [74]. In our case, the configuration of the anterior tentorial pit (character 50 in electronic supplementary material, table S4), the presence of an anterior mandibular joint (char 68), and the configuration of the posterior mandibular joint (char 71) may constitute such plesiomorphic characters which are, according to our data, mechanically interdependent on each other and thus show *concerted plesiomorphy* [64]. Concerted plesiomorphy—the retention of ancestral states in groups of characters—is a term introduced as the essential effect underlying phylogenetic niche conservatism [75–78]. Thus, with a biomechanical testing of character interdependency we should also be able to better explain the morphological basis of phylogenetic niche conservatism [77].

The biomechanical assessment of convergence is still at its infancy. There are only a handful of studies simulating the mechanical behaviour of insect body parts [56,57,79]. By contrast, the mechanical analysis of vertebrate body parts is at an advanced stage with many studies using FEA [35,80–82] and to a minor extent the combination of FEA with MDA [15,34,83,84]. In fact biomechanical studies in

vertebrates altered our understanding of the evolution in seemingly well-studied groups [82,85]. The crucial factor in our view is to use approaches resulting in objective parameters for assessment of character evolution. Combining biomechanical simulation techniques with morphological phylogenetics is certainly a promising avenue to better understand the phenotypic evolution of single traits, as well as whole character complexes under mechanical constraints in a diverse range of lifeforms.

Authors' contributions. A.B. and M.J.F. designed the study; A.B. conducted the experiments; A.B., P.J.W. and R.H. analysed the data. All authors wrote the manuscript and approved its final version.

Competing interests. The authors declare that they have no competing interests.

Funding. Scanning was financed by DESY (proposal no. I-20090211 and I-20100029) which is gratefully acknowledged. Development of VOX-FE2 was supported by EPSRC grant nos EP/1006745/1 and EP/1006753/1, and the embedded CSE programme of the ARCHER UK National Supercomputing Service, project codes eCSE04-11 and eCSE01-15. A.B. was financed by a research fellowship of the Deutsche Forschungsgemeinschaft (DFG ID: BL 1355/1-1).

Acknowledgements. Fabian Wilde and Felix Beckmann (both HZG/DESY) provided excellent support at the synchrotron facilities. Karen Meusemann and Björn M. von Reumont assisted during the SR-μCT experiments. Liam J. Revell helped with the implementation of the fitPagel function, the constant information flow he provides on his phytools blog is gratefully acknowledged. Bernhard Misof is thanked for useful comments to an earlier version of this paper and for his support to A.B.

References

1. Kjer KM, Simon C, Yavorskaya M, Beutel RG. 2016 Progress, pitfalls and parallel universes: a history of insect phylogenetics. *J. R. Soc. Interface* **13**, 20160363. (doi:10.1098/rsif.2016.0363)
2. Grimaldi D, Engel MS. 2005 *Evolution of the insects*. Cambridge, UK: Cambridge University Press.
3. Misof B *et al.* 2014 Phylogenomics resolves the timing and pattern of insect evolution. *Science* **346**, 763–767. (doi:10.1126/science.1257570)
4. Medved V, Marden JH, Fescemyer HW, Der JP, Liu J, Mahfooz N, Popadić A. 2015 Origin and diversification of wings: insights from a neopteran insect. *Proc. Natl Acad. Sci. USA* **112**, 15 946–15 951. (doi:10.1073/pnas.1509517112)
5. Hovmöller R, Pape T, Källersjö M. 2002 The Palaeoptera problem: basal pterygote phylogeny inferred from 18S and 28S rDNA sequences. *Cladistics* **18**, 313–323. (doi:10.1111/j.1096-0031.2002.tb00153.x)
6. Klass K. 2009 A critical review of current data and hypotheses on hexapod phylogeny. *Proc. Arthropodan Embryol. Soc. Jpn*. **43**, 3–22.
7. Kristensen NP. 1981 Phylogeny of insect orders. *Annu. Rev. Entomol*. **26**, 135–157. (doi:10.1146/annurev.en.26.010181.001031)
8. Whitfield JB, Kjer KM. 2008 Ancient rapid radiations of insects: challenges for phylogenetic analysis. *Annu. Rev. Entomol*. **53**, 449–472. (doi:10.1146/annurev.ento.53.103106.093304)
9. Thomas JA, Trueman JWH, Rambaut A, Welch JJ. 2013 Relaxed phylogenetics and the Palaeoptera problem: resolving deep ancestral splits in the insect phylogeny. *Syst. Biol*. **62**, 285–297. (doi:10.1093/sysbio/sys093)
10. Staniczek AH. 2000 The mandible of silverfish (Insecta: Zygentoma) and mayflies (Ephemeroptera): its morphology and phylogenetic significance. *Zool. Anz*. **239**, 147–178.
11. Staniczek AH. 2001 Der Larvenkopf von Oniscigaster wakefieldi McLachlan, 1873 (Insecta: Ephemeroptera: Oniscigastridae). Ein Beitrag zur vergleichenden Anatomie und Phylogenie der Eintagsfliegen. PhD thesis, Eberhard-Karls-Universität Tübingen.
12. Blanke A, Wipfler B, Letsch H, Koch M, Beckmann F, Beutel R, Misof B. 2012 Revival of Palaeoptera—head characters support a monophyletic origin of Odonata and Ephemeroptera (Insecta). *Cladistics* **28**, 560–581. (doi:10.1111/j.1096-0031.2012.00405.x)
13. Liu J, Shi J, Fitton LC, Phillips R, O'Higgins P, Fagan MJ. 2012 The application of muscle wrapping to voxel-based finite element models of skeletal structures. *Biomech. Model. Mechanobiol*. **11**, 35–47. (doi:10.1007/s10237-011-0291-5)
14. Moazen M, Curtis N, O'Higgins P, Evans SE, Fagan MJ. 2009 Biomechanical assessment of evolutionary changes in the lepidosaurian skull. *Proc. Natl Acad. Sci. USA* **106**, 8273–8277. (doi:10.1073/pnas.0813156106)
15. Moazen M, Curtis N, Evans SE, O'Higgins P, Fagan MJ. 2008 Combined finite element and multibody dynamics analysis of biting in a *Uromastyx hardwickii* lizard skull. *J. Anat*. **213**, 499–508. (doi:10.1111/j.1469-7580.2008.00980.x)
16. Betz O, Wegst U, Weide D, Heethoff M, Helfen L, Lee W-K, Cloetens P. 2007 Imaging applications of synchrotron X-ray phase-contrast microtomography in biological morphology and biomaterials science. I. General aspects of the technique and its advantages in the analysis of millimetre-sized arthropod structure. *J. Microsc*. **227**, 51–71. (doi:10.1111/j.1365-2818.2007.01785.x)
17. Hörnschemeyer T, Beutel RG, Pasop F. 2002 Head structures of *Priacma serrata* Leconte (Coleptera, Archostemata) inferred from X-ray tomography. *J. Morphol*. **252**, 298–314. (doi:10.1002/jmor.1107)
18. Wipfler B, Wieland F, DeCarlo F, Hörnschemeyer T. 2012 Cephalic morphology of *Hymenopus coronatus* (Insecta: Mantodea) and its phylogenetic implications. *Arthropod Struct. Dev*. **41**, 87–100. (doi:10.1016/j.asd.2011.06.005)
19. Friedemann K, Wipfler B, Bradler S, Beutel RG. 2012 On the head morphology of Phyllium and the phylogenetic relationships of Phasmatodea (Insecta). *Acta Zool*. **93**, 184–199. (doi:10.1111/j.1463-6395.2010.00497.x)
20. Romeis B. 1989 *Mikroskopische Technik*. München, Germany: Urban & Schwarzenberg.
21. Yushkevich PA, Piven J, Hazlett HC, Smith RG, Ho S, Gee JC, Gerig G. 2006 User-guided 3D active contour segmentation of anatomical structures: significantly improved efficiency and reliability. *Neuroimage* **31**, 1116–1128. (doi:10.1016/j.neuroimage.2006.01.015)
22. Curtis N, Jones MEH, Lappin AK, O'Higgins P, Evans SE, Fagan MJ. 2010 Comparison between in vivo and theoretical bite performance: using multi-body modelling to predict muscle and bite forces in a reptile skull. *J. Biomech*. **43**, 2804–2809. (doi:10.1016/j.jbiomech.2010.05.037)
23. Curtis N, Jones MEH, Evans SE, O'Higgins P, Fagan MJ. 2013 Cranial sutures work collectively to distribute strain throughout the reptile skull. *J. R. Soc. Interface* **10**, 20130442. (doi:10.1098/rsif.2013.0442)
24. Curtis N, Witzel U, Fagan MJ. 2014 Development and three-dimensional morphology of the zygomaticotemporal suture in primate skulls. *Folia Primatol. (Basel)* **85**, 77–87. (doi:10.1159/000357526)
25. Watson PJ, Gröning F, Curtis N, Fitton LC, Herrel A, McCormack SW, Fagan MJ. 2014 Masticatory biomechanics in the rabbit: a multi-body dynamics analysis. *J. R. Soc. Interface* **11**, 20140564. (doi:10.1098/rsif.2014.0564)
26. Blanke A, Greve C, Mokso R, Beckmann F, Misof B. 2013 An updated phylogeny of Anisoptera including formal convergence analysis of morphological characters. *Syst. Entomol*. **38**, 474–490. (doi:10.1111/syen.12012)
27. Pringle JWS. 1967 The contractile mechanism of insect fibrillar muscle. *Prog. Biophys. Mol. Biol*. **17**, 1–12. (doi:10.1016/0079-6107(67)90003-X)
28. Ellington CP. 1985 Power and efficiency of insect flight muscle. *J. Exp. Biol*. **115**, 293–304.
29. Granzier HL, Wang K. 1993 Passive tension and stiffness of vertebrate skeletal and insect flight muscles: the contribution of weak cross-bridges and elastic filaments. *Biophys. J*. **65**, 2141–2159. (doi:10.1016/S0006-3495(93)81262-1)

30. Herzog W, Binding P. 1992 Predictions of antagonistic muscular activity using nonlinear optimization. *Math. Biosci*. **111**, 217–229. (doi:10.1016/0025-5564(92)90071-4)
31. Herzog W. 2007 In *Biomechanics of the musculo-skeletal system* (eds BM Nigg, W Herzog). Chichester, UK: John Wiley & Sons, Ltd.
32. Curtis N, Jones MEH, Evans SE, Shi J, O'Higgins P, Fagan MJ. 2010 Predicting muscle activation patterns from motion and anatomy: modelling the skull of Sphenodon (Diapsida: Rhynchocephalia). *J. R. Soc. Interface R. Soc*. **7**, 153–160. (doi:10.1098/rsif.2009.0139)
33. David S, Funken J, Potthast W, Blanke A. 2016 Musculoskeletal modeling of the dragonfly mandible system as an aid to understanding the role of single muscles in an evolutionary context. *J. Exp. Biol*. **219**, 1041–1049. (doi:10.1242/jeb.132399)
34. Gröning F, Jones MEH, Curtis N, Herrel A, O'Higgins P, Evans SE, Fagan MJ. 2013 The importance of accurate muscle modelling for biomechanical analyses: a case study with a lizard skull. *J. R. Soc. Interface* **10**, 20130216. (doi:10.1098/rsif.2013.0216)
35. Gröning F, Fagan M, O'higgins P. 2012 Modeling the human mandible under masticatory loads: Which input variables are important? *Anat. Rec. Adv. Integr. Anat. Evol. Biol*. **295**, 853–863. (doi:10.1002/ar.22455)
36. Blanke A, Schmitz H, Dutel H, Patera A, Fagan M. 2016 Biomechanical trends in dragonfly mandibles superpose deep level systematic relationships but support the monophyly of major families. *J. R. Soc. Interface*.
37. Vincent JFV, Wegst UGK. 2004 Design and mechanical properties of insect cuticle. *Arthropod Struct. Dev*. **33**, 187–199. (doi:10.1016/j.asd.2004.05.006)
38. Hillerton JE, Reynolds SE, Vincent JFV. 1982 On the indentation hardness of insect cuticle. *J. Exp. Biol*. **96**, 45–52.
39. Revell LJ. 2012 phytools: an R package for phylogenetic comparative biology (and other things). *Methods Ecol. Evol*. **3**, 217–223. (doi:10.1111/j.2041-210X.2011.00169.x)
40. Paradis E, Claude J, Strimmer K. 2004 APE: analyses of phylogenetics and evolution in R language. *Bioinformatics* **20**, 289–290. (doi:10.1093/bioinformatics/btg412)
41. Popescu A-A, Huber KT, Paradis E. 2012 ape 3.0: New tools for distance-based phylogenetics and evolutionary analysis in R. *Bioinforma. Oxf. Engl*. **28**, 1536–1537. (doi:10.1093/bioinformatics/bts184)
42. Harmon LJ, Weir JT, Brock CD, Glor RE, Challenger W. 2008 GEIGER: investigating evolutionary radiations. *Bioinformatics* **24**, 129–131. (doi:10.1093/bioinformatics/btm538)
43. Pagel M. 1994 Detecting correlated evolution on phylogenies: a general method for the comparative analysis of discrete characters. *Proc. R. Soc. Lond. B* **255**, 37–45. (doi:10.1098/rspb.1994.0006)
44. Wipfler B, Machida R, Müller B, Beutel RG. 2011 On the head morphology of Grylloblattodea (Insecta) and the systematic position of the order, with a new nomenclature for the head muscles of Dicondylia. *Syst. Entomol*. **36**, 241–266. (doi:10.1111/j.1365-3113.2010.00556.x)
45. R Core Team. 2014 *R: a language and environment for statistical computing. R Foundation for Statistical Computing*. Vienna, Austria: R Foundation for Statistical Computing. (http://www.R-project.org)
46. Goloboff PA, Farris JS, Nixon KC. 2008 TNT, a free program for phylogenetic analysis. *Cladistics* **24**, 774–786. (doi:10.1111/j.1096-0031.2008.00217.x)
47. Ronquist F *et al.* 2012 MrBayes 3.2: Efficient Bayesian phylogenetic inference and model choice across a large model space. *Syst. Biol*. **61**, 539–542. (doi:10.1093/sysbio/sys029)
48. Beutel RG *et al.* 2011 Morphological and molecular evidence converge upon a robust phylogeny of the megadiverse Holometabola. *Cladistics* **27**, 341–355. (doi:10.1111/j.1096-0031.2010.00338.x)
49. Blanke A, Koch M, Wipfler B, Wilde F, Misof B. 2014 Head morphology of *Tricholepidion gertschi* indicates monophyletic Zygentoma. *Front. Zool*. **11**, 16. (doi:10.1186/1742-9994-11-16)
50. Cox PG, Fagan MJ, Rayfield EJ, Jeffery N. 2011 Finite element modelling of squirrel, guinea pig and rat skulls: using geometric morphometrics to assess sensitivity. *J. Anat*. **219**, 696–709. (doi:10.1111/j.1469-7580.2011.01436.x)
51. Tseng ZJ, Mcnitt-Gray JL, Flashner H, Wang X, Enciso R, Carpenter K. 2011 Model sensitivity and use of the comparative finite element method in mammalian jaw mechanics: mandible performance in the gray wolf. *PLoS ONE* **6**, e19171. (doi:10.1371/journal.pone.0019171)
52. David S, Funken J, Potthast W, Blanke A. 2016 Musculoskeletal modelling under an evolutionary perspective: deciphering the role of single muscle regions in closely related insects. *J. R. Soc. Interface* **13**, 20160675. (doi:10.1098/rsif.2016.0675)
53. Beutel RG, Friedrich F, Ge SQ, Yang XK. 2014 *Insect Morphology and Phylogeny*. Berlin, Germany: De Gruyter.
54. Paul J. 2001 Mandible movements in ants. *Comp. Biochem. Physiol. A. Mol. Integr. Physiol*. **131**, 7–20. (doi:10.1016/S1095-6433(01)00458-5)
55. Paul J, Gronenberg W. 1999 Optimizing force and velocity: mandible muscle fibre attachments in ants. *J. Exp. Biol*. **202**, 797–808.
56. Goyens J, Soons J, Aerts P, Dirckx J. 2014 Finite-element modelling reveals force modulation of jaw adductors in stag beetles. *J. R. Soc. Interface* **11**, 20140908. (doi:10.1098/rsif.2014.0908)
57. Goyens J, Dirckx J, Dierick M, Hoorebeke LV, Aerts P. 2014 Biomechanical determinants of bite force dimorphism in *Cyclommatus metallifer* stag beetles. *J. Exp. Biol*. **217**, 1065–1071. (doi:10.1242/jeb.091744)
58. von Lieven AF. 2000 The transformation from monocondylous to dicondylous mandibles in the Insecta. *Zool. Anz*. **239**, 139–146.
59. Anderson PSL, Friedman M, Brazeau MD, Rayfield EJ. 2011 Initial radiation of jaws demonstrated stability despite faunal and environmental change. *Nature* **476**, 206–209. (doi:10.1038/nature10207)
60. Fujiwara S, Kawai H. 2016 Crabs grab strongly depending on mechanical advantages of pinching and disarticulation of chela. *J. Morphol*. **277**, 1259–1272. (doi:10.1002/jmor.20573)
61. Sakamoto M. 2010 Jaw biomechanics and the evolution of biting performance in theropod dinosaurs. *Proc. R. Soc. B* **277**, 3327–3333. (doi:10.1098/rspb.2010.0794)
62. Weihmann T, Reinhardt L, Weißing K, Siebert T, Wipfler B, Gronenberg W. 2015 Fast and powerful: biomechanics and bite forces of the mandibles in the American cockroach *Periplaneta americana*. *PLoS ONE* **10**, e0141226. (doi:10.1371/journal.pone.0141226)
63. Blanke A, Greve C, Wipfler B, Beutel RG, Holland BR, Misof B. 2013 The identification of concerted convergence in insect heads corroborates Palaeoptera. *Syst. Biol*. **62**, 250–263. (doi:10.1093/sysbio/sys091)
64. Patterson TB, Givnish TJ. 2002 Phylogeny, concerted convergence, and phylogenetic niche conservatism in the core lilliales: insights from rbcL and ndhF sequence data. *Evolution* **56**, 233–252. (doi:10.1554/0014-3820(2002)056[0233:PCCAPN]2.0.CO;2)
65. Givnish TJ *et al.* 2005 Repeated evolution of net venation and fleshy fruits among monocots in shaded habitats confirms *a priori* predictions: evidence from an ndhF phylogeny. *Proc. R. Soc. B* **272**, 1481–1490. (doi:10.1098/rspb.2005.3067)
66. Givnish TJ *et al.* 2006 Phylogenetic relationships of monocots based on the highly informative plastid gene ndhf: evidence for widespread concerted convergence. *Aliso* **22**, 28–51.
67. Holland BR, Spencer HG, Worthy TH, Kennedy M. 2010 Identifying cliques of convergent characters: concerted evolution in the cormorants and shags. *Syst. Biol*. **59**, 433–445. (doi:10.1093/sysbio/syq023)
68. Baker AJ, Haddrath O, McPherson JD, Cloutier A. 2014 Genomic support for a Moa–Tinamou clade and adaptive morphological convergence in flightless ratites. *Mol. Biol. Evol*. **31**, 1686–1696. (doi:10.1093/molbev/msu153)
69. Felsenstein J. 1985 Phylogenies and the comparative method. *Am. Nat*. **125**, 1–15. (doi:10.1086/284325)
70. Baum DA, Larson A. 1991 Adaptation reviewed: a phylogenetic methodology for studying character macroevolution. *Syst. Zool*. **40**, 1–18. (doi:10.2307/2992218)
71. Givnish TJ, Sytsma KJ. 1997 Consistency, characters, and the likelihood of correct phylogenetic inference. *Mol. Phylogenet. Evol*. **7**, 320–330. (doi:10.1006/mpev.1997.0409)
72. Schwenk K, Wagner GP. 2001 Function and the evolution of phenotypic stability: connecting pattern to process. *Am. Zool*. **41**, 552–563. (doi:10.1093/icb/41.3.552)
73. Wake DB, Roth G, Wake MH. 1983 On the problem of stasis in organismal evolution. *J. Theor.*

Biol. **101**, 211–224. (doi:10.1016/0022-5193(83)90335-1)
74. Hansen TF. 1997 Stabilizing selection and the comparative analysis of adaptation. *Evolution* **51**, 1341–1351. (doi:10.2307/2411186)
75. Pyron RA, Costa GC, Patten MA, Burbrink FT. 2015 Phylogenetic niche conservatism and the evolutionary basis of ecological speciation. *Biol. Rev. Camb. Philos. Soc*. **90**, 1248–1262. (doi:10.1111/brv.12154)
76. Losos JB. 2008 Phylogenetic niche conservatism, phylogenetic signal and the relationship between phylogenetic relatedness and ecological similarity among species. *Ecol. Lett*. **11**, 995–1003. (doi:10.1111/j.1461-0248.2008.01229.x)
77. Cooper N, Jetz W, Freckleton RP. 2010 Phylogenetic comparative approaches for studying niche conservatism: comparative approaches for niche conservatism. *J. Evol. Biol*. **23**, 2529–2539. (doi:10.1111/j.1420-9101.2010.02144.x)
78. Wiens JJ, Graham CH. 2005 Niche conservatism: integrating evolution, ecology, and conservation biology. *Annu. Rev. Ecol. Evol. Syst*. **36**, 519–539. (doi:10.1146/annurev.ecolsys.36.102803.095431)
79. Hörnschemeyer T, Bond J, Young PG. 2013 Analysis of the functional morphology of mouthparts of the beetle *Priacma serrata*, and a discussion of possible food sources. *J. Insect Sci*. **13**, 1–14. (doi:10.1673/031.013.12601)
80. Dumont ER, Piccirillo J, Grosse IR. 2005 Finite-element analysis of biting behavior and bone stress in the facial skeletons of bats. *Anat. Rec. A. Discov. Mol. Cell. Evol. Biol*. **283A**, 319–330. (doi:10.1002/ar.a.20165)
81. Kupczik K, Dobson CA, Fagan MJ, Crompton RH, Oxnard CE, O'Higgins P. 2007 Assessing mechanical function of the zygomatic region in macaques: validation and sensitivity testing of finite element models. *J. Anat*. **210**, 41–53. (doi:10.1111/j.1469-7580.2006.00662.x)
82. Piras P, Maiorino L, Teresi L, Meloro C, Lucci F, Kotsakis T, Raia P. 2013 Bite of the cats: relationships between functional integration and mechanical performance as revealed by mandible geometry. *Syst. Biol*. **62**, 878–900. (doi:10.1093/sysbio/syt053)
83. Bright JA, Gröning F. 2011 Strain accommodation in the zygomatic arch of the pig: a validation study using digital speckle pattern interferometry and finite element analysis. *J. Morphol*. **272**, 1388–1398. (doi:10.1002/jmor.10991)
84. Curtis N, Jones MEH, Shi J, O'Higgins P, Evans SE, Fagan MJ. 2011 Functional relationship between skull form and feeding mechanics in *Sphenodon*, and implications for diapsid skull development. *PLoS ONE* **6**, e29804. (doi:10.1371/journal.pone.0029804)
85. Cunningham JA, Rahman IA, Lautenschlager S, Rayfield EJ, Donoghue PCJ. 2014 A virtual world of paleontology. *Trends Ecol. Evol*. **29**, 347–357. (doi:10.1016/j.tree.2014.04.004)